Thermochimica Acta 512 (2011) 129–133

Contents lists available at ScienceDirect

Thermochimica Acta

journal homepage: www.elsevier.com/locate/tca

Thermodynamic modeling of mineralogical phases formed by continuous casting powders

Julio Romo-Castañeda, Alejandro Cruz-Ramírez*, Antonio Romero-Serrano, Marissa Vargas-Ramírez, Manuel Hallen-López

Metallurgy and Materials Department, Instituto Politecnico Nacional-ESIQIE, Apdo. P. 118-431, 07051 Mexico D.F., Mexico

ARTICLE INFO

Article history:
Received 2 July 2010
Received in revised form
10 September 2010
Accepted 15 September 2010
Available online 21 September 2010

Keywords:
Thermodynamic
Flux
Solidification
Mineralogical phases
Cuspidine

ABSTRACT

A great amount of mineralogical phases were predicted and represented in stability phase diagrams, which were obtained by the use of the thermodynamic software FACTSage considering both the chemical composition and the melting temperature of the mould flux. Melting-solidification tests on commercial mould flux glasses for thin slab casting of steel revealed the existence of cuspidine ($Ca_4Si_2O_7F_2$) as the main mineralogical phase formed during the flux solidification by X-ray powder diffraction (XRD). This phase directly influences the heat transfer phenomena from the strand to the mould and it is obtained with higher fluorite content (22% CaF_2). Cuspidine is desirable only in fluxes to produce medium carbon (included peritectic grade) steels, because it reduces the heat flux from the strand to the mould, thus controlling the shrinkage rate during the flux solidification. The experimental results are in agreement with those obtained by the thermodynamic software. The stability phase diagrams could be used as an important tool in the flux design for continuous casting process.

1. Introduction

Mould powders must fulfill several functions during the continuous casting of steel. They play an important role in the surface quality of the steel product and in the overall efficiency of the continuous casting process control [1]. More recently, high speed continuous casting was developed in order to improve productivity and conserve energy in the continuous casting of steel slabs [2,3]. Improvement in mould lubrication is therefore crucial for efficient high-speed casting, and mould powder has been developed for this purpose. Thin slab casting powders are mixtures of oxides generally based on the SiO_2–CaO–CaF_2–Na_2O system. Three to six percent graphite is usually added to control the melting characteristics and to improve the thermal insulation properties of the fluxes [4]. The chemical composition and the physical form of the flux can control the melting temperature, melting rate, viscosity and surface tension of the flux. It has been found that viscosity and the melting temperature of the mould flux are increased when silica and alumina are added to the original composition of mould fluxes [5–7]. The size of the silicate or aluminosilicate network in casting powders or slags become larger with increasing SiO_2 and Al_2O_3 contents, hence their mobility decreases resulting in a higher viscosity. The addition of metal oxides, such as Na_2O, leads to the breakdown of the silicate network, resulting in lower viscosity. There are considerable variations in the constituents used by powder manufacturers, and when the casting powders are heated the constituents react to form different mineralogical phases. The mineralogical constitution of the powder is of particular importance since it affects the melting rate of the powder, the lubrication characteristics and the heat transfer between the strand and the mould, thus impacting decisively the casting performance [5,6]. Mills [7] represented the chemical composition of casting powders by a pseudoternary system. Grieveson et al. [5] identified the phases formed in a wide range of chemical compositions by controlling the rate of melting of the casting powder and an attempt to represent the mineralogical phases in a phase diagram was also made. Hiromoto et al. [8] identified the phases formed in five synthetic fluxes at various temperatures between 773 K and the melting point after quenching and analyzing by X-ray diffraction. They observed that above 1073 K the original constituents were replaced by more complex mixtures of oxides or oxyfluorides and that the concentrations of those complex compounds increased with temperature. The most abundant phases in the fluxes at higher temperatures were cuspidine ($Ca_4Si_2O_7F_2$), and a pectolite phase ($Na_2CaSi_3O_8$) with smaller amounts of pseudowollastonite ($CaSiO_3$). When alumina was added to the powder, anorthite ($CaAl_2Si_2O_8$), gehlenite ($Ca_2Al_2SiO_7$), and nepheline ($NaAlSiO_4$) were also formed [8,9]. The kind of mineralogical phases formed affects the melting temperature and consequently the melting rate of the powder. The phases formed when a liquid flux

* Corresponding author. Tel.: +52 55 5729 6000x54202; fax: +52 55 57296000x55270.
E-mail address: alcruzr@ipn.mx (A. Cruz-Ramírez).

0040-6031/$ – see front matter © 2010 Elsevier B.V. All rights reserved.
doi:10.1016/j.tca.2010.09.014

Table 1
Chemical composition of commercial mould powders.

Chemical compounds	Mould fluxes (wt%)	
	P1	P2
SiO_2	27.04	25.51
CaO	28.85	29.71
MgO	2.06	1.97
Al_2O_3	2.08	2.09
Fe_2O_3	0.59	0.41
MnO	0.04	2.92
Na_2O	11.7	9.36
K_2O	0.73	0.38
CaF_2	21.84	22.1
C_{total}	4.97	5.04
H_2O	0.40	0.50

solidifies also have been identified by annealing glassy slag films formed between the mould and the strand [9]. One of the most effective means to decrease the heat flux is to use highly crystallizing mould fluxes. A crystalline layer in the slag film yields larger thermal resistance by producing air gap at the flux/mould interface. Cuspidine ($Ca_4Si_2O_7F_2$) is one of the most important compounds crystallized in mould flux film during thin slab casting process. Watanabe et al. [9] determined the primary crystallization field and the melting temperature of cuspidine. Fukuyama et al. [11] obtained experimentally the Gibbs energy of formation of cuspidine with the electromotive force method. Furthermore, the mineralogical phases formed during the melting and solidification of the flux are difficult to be expressed accurately in a phase diagram because of its complication with many phase formed. In the present work, stability phase diagrams of mineralogical species were obtained at different chemical compositions and temperatures with the thermodynamic software FACTSage [12] in order to estimate the melting-solidification behavior of the mould flux.

2. Experimental

Two commercial mould flux glasses used in an integrated Mexican steelmaking shop were characterized. Table 1 shows the chemical composition of these powders. Both powders are used to produce medium carbon (0.07–0.1% C) and peritectic (0.09–0.15% C) steel grades. The fluxes were compacted with a load of 1 ton within a stainless steel die to produce small cylinder flux samples of 6 mm diameter and 10 mm height. These samples are heated to their fluidity temperature, which were previously determined. This melting solidification tests involves the comparison of the height of a cylindrical flux sample (6 mm diameter and 10 mm height), with those of two different reference alumina tubes (8 and 5 mm height, respectively) as was reported by Cruz et al. [13]. In order to know the degree of crystallinity, the fluxes were heated up to 1573 K and then cooled at two different rates. In one experiment, the fluxes were cooled slowly inside the furnace and in the other test they were rapidly cooled by pouring the molten flux on a copper plate. Finally, the glass frit obtained was crushed and analyzed in an X-ray SIEMENS D 5000 diffractometer with monochromatic Cu Kα radiation.

3. Thermodynamic modeling

FACTSage [12] was used to determine the concentration of the different chemical species once they reach the chemical equilibrium state. The user gives the initial amount of chemical species, the temperature and the pressure of the system (usually 1 atm), then the program calculates the most stable species with the Gibbs free energy minimization method. FACTSage [12] does not include cuspidine in its database, so this phase was incorporated in a database considering the Gibbs free energy of formation of cuspidine reported by Fukuyama et al. [11]. In order to obtain stability phase diagram of mineralogical phases, the flux chemical composition was fixed by a basicity ratio of 1. The basicity ratio was considered as ($CaO + MgO/SiO_2$) and ($CaO + MgO/SiO_2 + Al_2O_3$) to observe the alumina effect. The phase diagrams were obtained from 0 to 24% CaF_2 and from 0 to 12% Na_2O. The basicity ratio was selected according with the work reported by Kromhout et al. [14], where several fluxes for thin continuous slab casting with different chemical compositions were studied. According with the chemical species considered, the stability phase diagram is based in the SiO_2–Al_2O_3–CaO–MgO–CaF_2–Na_2O system, which almost includes the chemical composition of the whole commercial fluxes reported to produce thin slab castings of steel. The stability phase diagrams were evaluated to 1473, 1573 and 1673 K.

Table 2
Softening, melting and fluidity temperatures for the commercial fluxes.

Powder	Temperature (K)		
	Softening	Melting	Fluidity
P1	1238	1337	1371
P2	1271	1321	1375

4. Results

Table 2 shows the softening, melting and fluidity temperatures determined for each of the commercial fluxes studied. As can be observed, the mixtures P1 and P2, both possess high softening, melting and fluidity temperatures, as expected for powders used in medium and peritectic carbon steels. The XRD patterns of the tested fluxes are shown in Figs. 1 and 2 for fluxes P1 and P2, respectively. The powders as received show simple chemical compounds such as $CaCO_3$, C, CaF_2, Na_2CO_3. It is also observed the presence of pseudo-wollastonite ($CaSiO_3$), which appears in both fluxes as received. It is known that these chemical compounds are present in minerals like feldspars, clays, limestone, fluorspar and graphite [15]. Both fluxes show that a main transformation was carried out from the original compounds to form a new complex mineralogical phase when the fluxes were heated to 1573 K. The calculated phases obtained by FACTSage [12] considering the chemical composition and the temperature were represented in stability phase diagrams. Fig. 3 shows the stability phase diagram of the SiO_2–CaO–MgO–CaF_2–Na_2O system obtained considering a basicity index ($CaO + MgO/SiO_2$) = 1 and 1473 K. Fig. 4 shows the flux solidification behavior in the SiO_2–CaO–MgO–CaF_2–Na_2O system to a fixed chemical composition of 4% CaF_2 and 12% Na_2O (represented by an square in Fig. 3). Alumina is also added to the fluxes in lower proportions to increase the viscosity and the melting temperature of the mixture, Fig. 5 shows the stability phase diagram of the SiO_2–Al_2O_3–CaO–MgO–CaF_2–Na_2O system obtained considering a basicity index ($CaO + MgO/SiO_2 + Al_2O_3$) = 1 and 1273 K. In addition, Figs. 6 and 7 show the effect of increase the temperature to 1473 and 1673 K, respectively, in the mineralogical phase formation for the SiO_2–Al_2O_3–CaO–MgO–CaF_2–Na_2O system to a basicity index ($CaO + MgO/SiO_2 + Al_2O_3$) = 1.

5. Discussion

The main phase experimentally obtained in both fluxes at the temperature of 1573 K by XRD (Figs. 1 and 2) was the cuspidine ($Ca_4Si_2O_7F_2$). The quantity of cuspidine phase varied from one to another flux according to the original chemical composition of the fluxes. For the fluxes tested, the cooling velocity affects the formation of phases. For the slow cooled velocity, there were

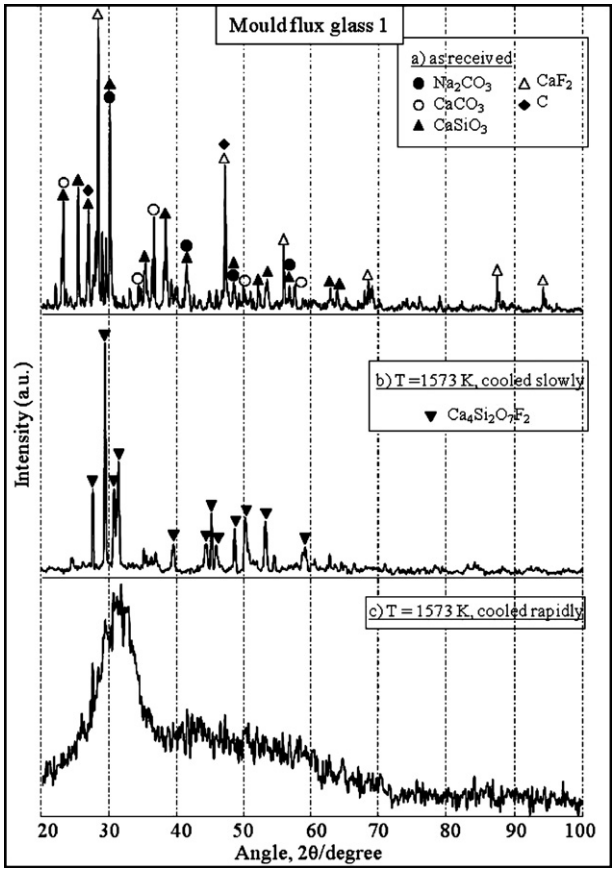

Fig. 1. XRD patterns of the P1 glass: (a) as received, (b) heat treated to 1573 K and cooled slowly and (c) heat treated to 1573 K and cooled rapidly.

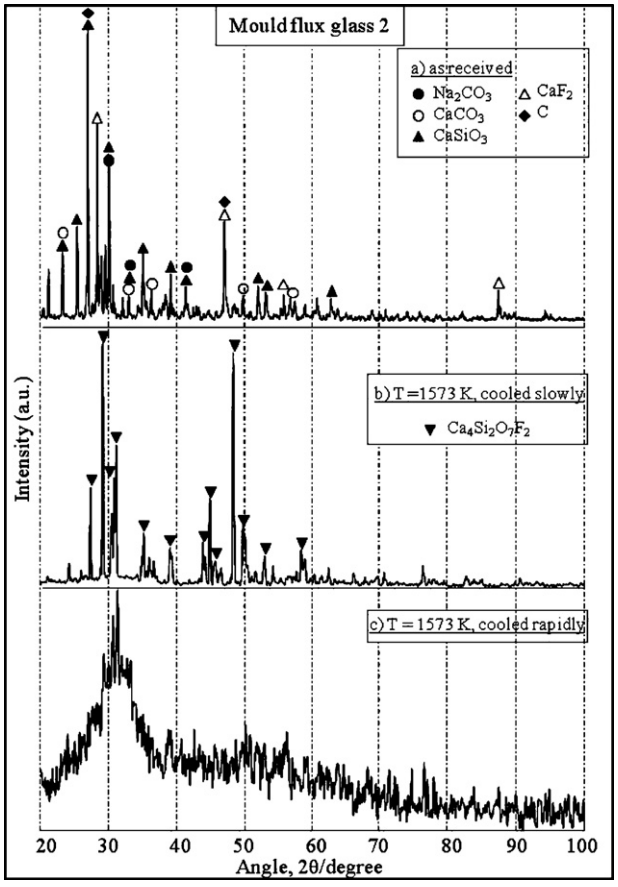

Fig. 2. XRD patterns of the P2 glass: (a) as received, (b) heat treated to 1573 K and cooled slowly and (c) heat treated to 1573 K and cooled rapidly.

whole transformations from the original compounds to cuspidine phase, whereas the fast cooled velocity does not obtain a crystalline phase. The amorphous phase detected could be present in the layer closer to the mould and increase the heat transfer from strand to mould. The phases identified with the thermodynamic prediction for the SiO_2–CaO–MgO–CaF_2–Na_2O system to 1473 K (Fig. 3) shows a wide variety of mineralogical phases which are: cuspidine ($Ca_4Si_2O_7F_2$), merwinite ($MgOCa_3O_3Si_2O_4$), akermanite ($Ca_2MgSi_2O_7$), pseudo-wollastonite ($CaSiO_3$) and Diopside ($CaMgSi_2O_6$), also simple chemical compounds were detected, these are: silica (SiO_2), fluorite (CaF_2) and a liquid phase. Fig. 3 does not show any mineralogical phase that contains sodium. In order to determine the flux solidification behavior and the possibility to form any mineralogical specie containing sodium, Fig. 4 shows at high temperature (1473 K) the formation of cuspidine and merwinite as is observed in Fig. 3 for this chemical composition (4% CaF_2 and 12% Na_2O), these solid phases represent 8.34% and the liquid phase is present in 91.66%, when the temperature decrease to 1273 K, the amount of solid phase is increased and appears two complex silicate of calcium and sodium, these are: $Na_2Ca_2Si_3O_9$ and $Na_4CaSi_3O_9$, this means that in Fig. 3, sodium is content in the liquid phase. At this point the liquid phase is reduced to 4%. Fig. 5 shows the effect of the alumina (Al_2O_3) addition to the SiO_2–CaO–MgO–CaF_2–Na_2O system, considering a basicity index ($CaO + MgO/SiO_2 + Al_2O_3$) = 1 and 1273 K. It is notorious the increasing in the amount of solid phases formed, new phases appears like: gehlenite ($Ca_2Al_2Si_2O_7$), anortite ($CaAl_2Si_2O_8$), spinel ($MgAl_2O_4$), monticellite ($CaOMgOSiO_2$) and forsterite (Mg_2SiO_4); the simple chemical compounds (SiO_2 and CaF_2) detected in Fig. 3 are not predicted for this conditions. When the temperature is increased the stability phase diagram of the SiO_2–Al_2O_3–CaO–MgO–CaF_2–Na_2O system shows an increase in the liquid phase and some solid phases still remain as cuspidine, merwinite fluorite, anortite and akermanite for 1473 K (Fig. 6). In Fig. 7 the stability phase diagram of the SiO_2–Al_2O_3–CaO–MgO–CaF_2–Na_2O system shows at 1673 K a large liquid region that contains solid phases with high melting point, these are the cuspidine, merwinite and fluorite. The experimental determination of cuspidine is in good agreement with the results reported by several authors [9,10,16] and also with the thermodynamic prediction by FACTSage [11] as can be shown in the stability phase diagrams obtained. Therefore, in both fluxes, the new mineralogical phases were formed before the complete melting of the powders. Cuspidine was found in both fluxes because in the original composition of the powders there was a considerable amount

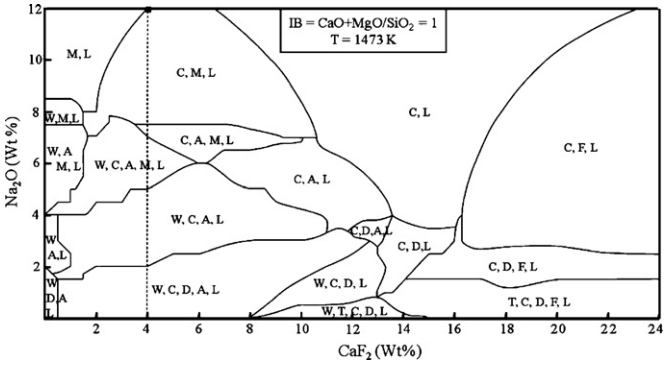

Fig. 3. Stability phase diagram of the SiO_2–CaO–MgO–CaF_2–Na_2O system to basicity index $CaO + MgO/SiO_2 = 1$ and 1473 K, where: (C) $Ca_4Si_2F_2O_7$; (F) CaF_2; (M) $MgOCa_3O_3Si_2O_4$; (A) $Ca_2MgSi_2O_7$; (W) $CaSiO_3$; (D) $CaMgSi_2O_6$; (T) SiO_2; (L) liquid.

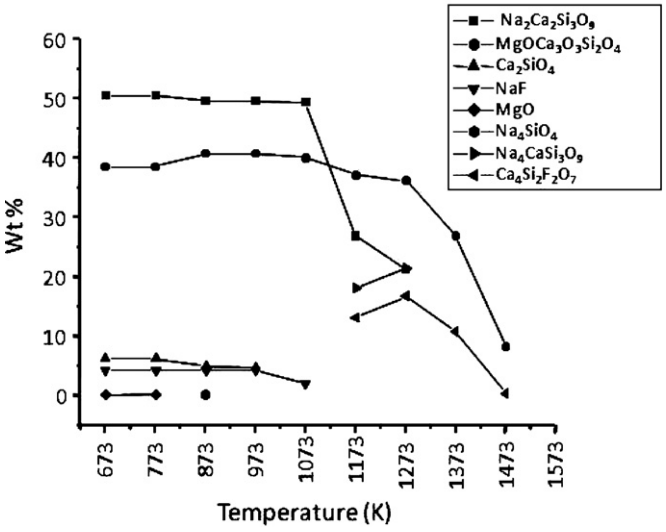

Fig. 4. Effect of the addition of 4% CaF_2 on the phases formation during solidification with a basicity index ($CaO + MgO/SiO_2$) = 1 and 12% Na_2O. Lines represent the weight % of each solid phase formed. The balance corresponds to % liquid in the system at each temperature.

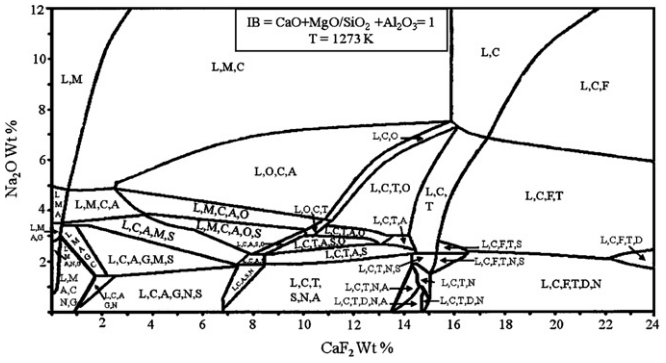

Fig. 5. Stability phase diagram of the SiO_2–Al_2O_3–CaO–MgO–CaF_2–Na_2O system to basicity index ($CaO + MgO/SiO_2 + Al_2O_3$) = 1 and 1273 K, where: (C) $Ca_4Si_2F_2O_7$; (F) CaF_2; (M) $MgOCa_3O_3Si_2O_4$; (A) $Ca_2MgSi_2O_7$; (D) $CaMgSi_2O_6$; (T) Mg_2SiO_4; (L) liquid; (G) $Ca_2Al_2SiO_7$; (N) $CaAl_2Si_2O_8$; (S) $MgAl_2O_4$; (O) $CaOMgOSiO_2$.

of CaF_2. According to the SiO_2–CaF_2–CaO ternary system [2,9], the cuspidine phase is stable below 1723 K. Therefore, cuspidine is useful to decrease the heat transfer from the strand to the mould in the earlier casting stages. Because process control of thin slab casting is more stringent, it is generally assumed that mould powder

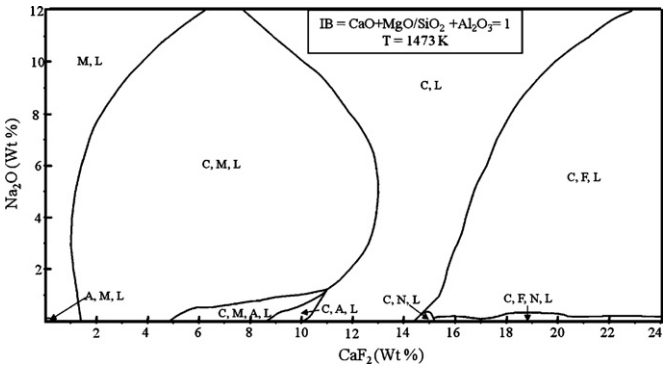

Fig. 6. Stability phase diagram of the SiO_2–Al_2O_3–CaO–MgO–CaF_2–Na_2O system to basicity index ($CaO + MgO/SiO_2 + Al_2O_3$) = 1 and 1473 K, where: (C) $Ca_4Si_2F_2O_7$; (F) CaF_2; (M) $MgOCa_3O_3Si_2O_4$; (A) $Ca_2MgSi_2O_7$; (L) liquid; (N) $CaAl_2Si_2O_8$.

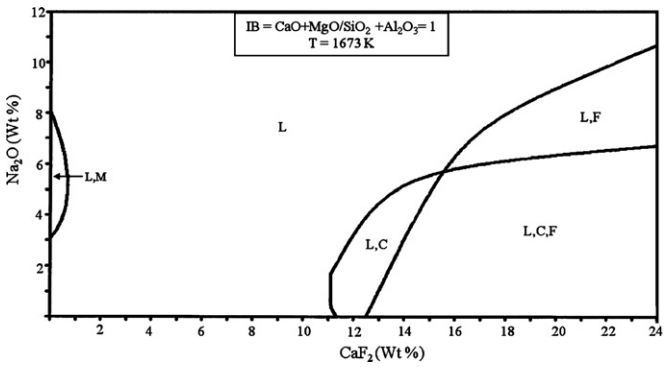

Fig. 7. Stability phase diagram of the SiO_2–Al_2O_3–CaO–MgO–CaF_2–Na_2O system to basicity index ($CaO + MgO/SiO_2 + Al_2O_3$) = 1 and 1673 K, where: (C) $Ca_4Si_2F_2O_7$; (F) CaF_2; (M) $MgOCa_3O_3Si_2O_4$; (L) liquid.

properties become more critical. Basically, mould powders for thin slab casting have a high basicity from 1 to 1.2 [14]. It has been reported [14] that the slag mould basicity is not a key parameter in the observed mould behavior; however it is also know that the kind of mineralogical phases formed during the flux melting – solidification directly affects the melting temperature and consequently the melting rate of the powder. As was observed in the flux characterization, a design strategy to produce fluxes for thin slab casting is the addition of high quantities of fluorite (22% CaF_2) with alkali oxide (9–12% Na_2O) added as fluidizer to obtain cuspidine into a liquid phase to promote and adequate lubrication and heat removal during the initial casting stages of steel.

6. Conclusions

The mineralogical phases formed during the solidification of mould fluxes have an important role in the heat transfer from the strand to the continuous casting mould. For the thin slab casting process of steel is desirable to form cuspidine, which has a high melting point (1680 K) and acts as a thermal barrier. To form cuspidine, considerable amounts of CaF_2 and Na_2O are needed to add to the fluxes. The use of the thermodynamic software FACTSage shows a high degree of confidence in determining the main mineralogical phases formed in the fluxes. The cooling rate of the fluxes affects the formation of the mineralogical phases and may form amorphous phases in the layer flux closer to the liquid metal. The stability phase diagrams could be used as an important tool in the flux design for continuous casting process.

Acknowledgements

The authors wish to thank the Institutions CONACyT, SNI, COFAA and IPN for their permanent assistance to the Process Metallurgy Group at ESIQIE-Metallurgy and Materials Department.

References

[1] F. Chávez, A. Rodríguez, R. Morales, V. Tapia, 78th Steelmaking Conference ISS, 1995, pp. 679–686.
[2] M. Hanao, M. Kawamoto, T. Watanabe, ISIJ International 44 (5) (2004) 827–835.
[3] M. Kawamoto, K. Nakajima, T. Kanazawa, K. Nakai, ISIJ International 34 (7) (1994) 593–598.
[4] R. Scheel, W. Korte, Stahl und Eissen 107 (17) (1987) 781–787.
[5] P. Grieveson, S. Bagha, N. Machingawuta, K. Liddell, K.C. Mills, Ironmaking and Steelmaking 15 (4) (1988) 181–186.
[6] R. Bommaraju, Steelmaking Conference Proceedings, ISS-AIME, vol. 74, 1991, pp. 131–146.
[7] K.C. Mills, Ironmaking and Steelmaking 15 (4) (1988) 175–180.

[8] T. Hiromoto, R. Sato, T. Shima, Steelmaking Proceedings, AIME, vol. 62, 1979, pp. 40–47.
[9] T. Watanabe, H. Fukuyama, K. Nagata, ISIJ International 42 (5) (2002) 489–497.
[10] R.G. Hill, N. Da Costa, R.V. Law, Journal of Non-Crystalline Solids 351 (2005) 69–74.
[11] H. Fukuyama, H. Tabata, T. Oshima, K. Nagata, ISIJ International 44 (9) (2004) 1488–1493.
[12] C.W. Bale, A.D. Pelton, W.T. Thompson, Facility for the Analysis of Chemical Thermodynamics (FACTSage v 6.1), User's Guide, 2009.
[13] A. Cruz, F. Chávez, A. Romero, E. Palacios, Transactions of the Institution of Mining and Metallurgy Section C: Mineral Processing and Extractive Metallurgy 116 (1) (2007) 65–71.
[14] J. Kromhout, A. Kamperman, M. Kick, J. Trouw, VII International Conference on Molten, Slags, Fluxes and Salts, 2004, pp. 731–736.
[15] A. Cruz, F. Chávez, J.A. Romero, Revista de Metal Madrid 40 (2004) 39–45.
[16] A. Cruz, F. Chávez, A. Romero, E. Palacios, V. Arredondo, Journal of Materials Processing Technology 182 (1–3) (2007) 358–362.